

Copyright held by the IEEE. Url: [www.ieee.org](http://www.ieee.org)

DOI: 10.1109/LSP.2016.2614982

To cite this article: F. Bandiera, A. Coluccia, V. Dodde, A. Masciullo and G. Ricci, "CRLB for I/Q Imbalance Estimation in FMCW Radar Receivers," in *IEEE Signal Processing Letters*, vol. 23, no. 12, pp. 1707-1711, December 2016, doi: 10.1109/LSP.2016.2614982.

# CRLB for I/Q imbalance estimation in FMCW radar receivers

Francesco Bandiera, *Member, IEEE*, Angelo Coluccia, *Member, IEEE*, Vincenzo Dodde, Antonio Masciullo, and Giuseppe Ricci, *Senior Member, IEEE*

**Abstract**—This paper deals with estimation of gain and phase errors possibly present in FMCW radars. In particular, the CRLB of unbiased estimators of gain and phase errors in presence of nuisance parameters is computed. It is used as a reference for the performance of already proposed estimators (computed by Monte Carlo simulation).

**Index Terms**—FMCW radar, I/Q imbalance, CRLB.

## I. INTRODUCTION

**R**ADARS for automotive scenarios are typically frequency modulated continuous wave (FMCW) sensors due to computational power and cost concerns [1], [2], [3]. In automotive scenarios, target detection has to deal with multiple, possibly extended targets. The presence of non idealities makes the detection task even more challenging. For instance, this is the case of gain and phase errors in the computation of I and Q components that give rise to additional frequency terms, namely to image responses at frequencies that are the negative of the actual ones, and to correlated baseband noise. The problem has been dealt with in [4], [5], [6], [7], [8], [9]. In particular, [4], [5] present “a method to orthogonalize” the I and Q components by means of correction coefficients; such coefficients are derived from measurements of a test signal. In [6], [7], [8], [9] estimation of gain and phase errors is further addressed without using test signals. Compensation of I/Q imbalance is of relevant interest also in the context of direct conversion of wideband communication signals. The algorithms proposed in [10], [11] exploit the proper nature of complex communication waveforms. In fact, under quite reasonable assumptions, a composite intermediate frequency (IF) signal, consisting of multiple modulated IF carriers, is proper. Then, since I/Q imbalance can destroy signal properness, it is possible to compensate imbalance by recovering such a property. Remarkably, such solutions can handle the case of frequency-dependent I/Q imbalance that may come into play with large bandwidths. A modification of the above idea is also applied to compensate I/Q imbalance in FMCW radars; however, a notch filter is necessary to guarantee the proper nature of the complex envelope of the radar signal [12].

In the following, we compute the Cramér-Rao lower bound (CRLB) of unbiased estimators of gain and phase errors in

Copyright (c) 2015 IEEE. Personal use of this material is permitted. However, permission to use this material for any other purposes must be obtained from the IEEE by sending a request to pubs-permissions@ieee.org.

The authors are with the Dipartimento di Ingegneria dell’Innovazione, University of Salento, Lecce, Italy. Email: {name.surname}@unisalento.it

presence of nuisance parameters. In particular, we assume that the level of the bandpass noise at the input of the receiver together with the (deterministic) amplitude and phase of a single target echo are unknown parameters. Section II introduces the models for the involved quantities. Section III focuses on the computation of the CRLB while Section IV shows its relevance to assess the performance of already proposed estimators. Finally, Section V gives the conclusions of the paper.

## II. NOISE AND USEFUL SIGNAL MODELS

Assume an FMCW radar located at the origin of a Cartesian coordinate system. The radar transmits a continuous carrier modulated by a periodic function such as a triangular wave to provide range data [13]. The instantaneous transmitted frequency assumes the following expression over  $(0, T)$

$$f(t) = f_0 + \alpha t$$

where  $\alpha$  is the chirp rate and  $f_0$  the transmitted frequency at time  $t = 0$ . The phase of the carrier, over  $(0, T)$ , is given by

$$\phi(t) = 2\pi \int_0^t f(\tau) d\tau = 2\pi f_0 t + \pi \alpha t^2.$$

Figure 1 shows the zero IF quadrature transceiver typically used in FMCW radar applications.

The signal at the output of the local oscillator (LO) can be written as

$$l(t) = A_L \cos(2\pi f_0 t + \pi \alpha t^2).$$

The received signal (in presence of a single target within the surveillance region) is a delayed and attenuated version of the transmitted one. Supposing the target moves with constant velocity  $v$  along a radial trajectory, the range of the target to the radar at time  $t$ , say  $r(t)$ , is given by

$$r(t) = r_0 + vt$$

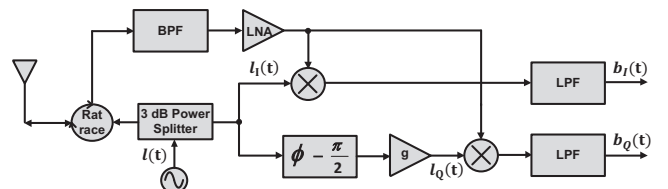


Fig. 1. Zero IF quadrature transceiver.

with  $r_0$  the range at  $t = 0$ . It follows that the received signal can be written as

$$s(t) = A_R \cos \left[ 2\pi f_0(t - \tau(t)) + \pi\alpha(t - \tau(t))^2 \right] + w(t)$$

where  $w(t)$  is the received noise and

$$\tau(t) = \frac{2r(t)}{c \left(1 + \frac{v}{c}\right)} \approx \frac{2r(t)}{c}$$

is the round trip delay with  $c$ , in turn, the speed of light.

If we take into account phase and amplitude errors, denoted by  $\phi$  and  $g$ , respectively, the two branches of the LO can be written as follows

$$\begin{aligned} l_I(t) &= \frac{A_L}{\sqrt{2}} \cos(2\pi f_0 t + \pi\alpha t^2) \\ l_Q(t) &= g \frac{A_L}{\sqrt{2}} \cos\left(2\pi f_0 t + \pi\alpha t^2 + \phi - \frac{\pi}{2}\right) \\ &= g \frac{A_L}{\sqrt{2}} \sin(2\pi f_0 t + \pi\alpha t^2 + \phi). \end{aligned}$$

The received signal  $s(t)$  is mixed with  $l_I(t)$  and  $l_Q(t)$ . After lowpass filtering, the  $I$  and  $Q$  components, in presence of a target echo, can be approximated as

$$\begin{aligned} b_I(t) &= 2a' \cos(2\pi f_T t + \theta) \\ &\quad + n_I(t) \\ b_Q(t) &= 2a'g \sin(2\pi f_T t + \theta + \phi) \\ &\quad + n_Q(t) \end{aligned}$$

where  $f_T = 2\frac{v}{c}f_0 + 2\alpha\frac{r_0}{c}$ ,  $\theta = 4\pi\frac{f_0 r_0}{c}$ , and  $a' = \frac{A_L A_R}{4\sqrt{2}}$ .

Suppose that the lowpass filters (LPFs) can be approximated by ideal filters with cut-off frequency equal to  $W > f_T$  and that the baseband signals are sampled with sampling frequency  $f_s = 1/T_s = 2W$ . The corresponding discrete-time signal is (approximately) given by

$$\begin{aligned} z(k) &= z_I(k) + jz_Q(k) \\ &= a' \left[ (1 - ge^{-j\phi})e^{-j(2\pi\nu_T k + \theta)} \right. \\ &\quad \left. + (1 + ge^{j\phi})e^{j(2\pi\nu_T k + \theta)} \right] \\ &\quad + n(k), \quad k = 0, \dots, N-1 \end{aligned} \quad (1)$$

where  $\nu_T = f_T T_s$  is the normalized frequency shift of the target,  $z_I(k) = b_I(kT_s)$ ,  $z_Q(k) = b_Q(kT_s)$ ,  $n(k) = n_I(kT_s) + jn_Q(kT_s)$ ,  $n_I(kT_s), n_Q(kT_s) \in \mathbb{R}$ . Equation (1) highlights the presence of the image response at frequency  $-\nu_T$  whether  $\phi \neq 0$  and/or  $g \neq 1$ . The random variables (rvs)  $n(k)$  are assumed jointly Gaussian and zero-mean; in particular, from the analysis in [8] it turns out that

$$\begin{aligned} E[n_I(rT_s)n_Q(sT_s)] &= g\sigma^2 \sin\phi \delta_{r,s} \\ E[n_I(rT_s)n_I(sT_s)] &= \sigma^2 \delta_{r,s} \\ E[n_Q(rT_s)n_Q(sT_s)] &= g^2 \sigma^2 \delta_{r,s} \end{aligned} \quad (2)$$

with  $\sigma^2 > 0$  a proper factor and  $\delta_{r,s}$  denoting, in turn, the Kronecker delta.

### III. COMPUTATION OF THE CRLB

The following proposition gives the expression of the CRLB for the problem at hand.

*Proposition 3.1:* Let  $\mathbf{y} = [\mathbf{y}^T(0) \dots \mathbf{y}^T(N-1)]^T$ , where  $\mathbf{y}(k) = [z_I(k) z_Q(k)]^T$  with

$$\begin{aligned} z_I(k) &= A \cos(2\pi\nu_T k + \theta) + n_I(kT_s), \\ z_Q(k) &= Ag \sin(2\pi\nu_T k + \theta + \phi) + n_Q(kT_s), \end{aligned}$$

$k = 0, \dots, N-1$ ,  $A = 2a'$ , and  $T$  the transpose operator. The noise terms  $n_I(kT_s)$ ,  $n_Q(kT_s)$ ,  $k = 0, \dots, N-1$ , are zero-mean, jointly Gaussian random sequences with statistical characterization given by Equations (2). Finally, denote by  $\mathbf{x} = [g \phi \sigma^2 A \theta]^T$  the parameter vector. The Fisher information matrix  $\mathbf{J}$  associated with the probability density function of  $\mathbf{y}$  is given by

$$\mathbf{J} = \frac{1}{2} \mathbf{A} + \mathbf{B} \quad (3)$$

where

$$\mathbf{A} = \begin{bmatrix} A_{11} & A_{12} & A_{13} & 0 & 0 \\ A_{12} & A_{22} & A_{23} & 0 & 0 \\ A_{13} & A_{23} & A_{33} & 0 & 0 \\ 0 & 0 & 0 & 0 & 0 \\ 0 & 0 & 0 & 0 & 0 \end{bmatrix}$$

and

$$\mathbf{B} = \begin{bmatrix} B_{11} & B_{12} & 0 & B_{14} & B_{15} \\ B_{12} & B_{22} & 0 & B_{24} & B_{25} \\ 0 & 0 & 0 & 0 & 0 \\ B_{14} & B_{24} & 0 & B_{44} & B_{45} \\ B_{15} & B_{25} & 0 & B_{45} & B_{55} \end{bmatrix}$$

with

$$\begin{aligned} A_{11} &= \frac{2N(2 - \sin^2 \phi)}{g^2 \cos^2 \phi}, A_{12} = -\frac{2N}{g} \tan \phi, A_{13} = \frac{2N}{\sigma^2 g}, \\ A_{22} &= \frac{2N(1 + \sin^2 \phi)}{\cos^2 \phi}, A_{23} = -\frac{2N}{\sigma^2} \tan \phi, A_{33} = \frac{2N}{\sigma^4}, \\ B_{11} &= \frac{A^2}{2\sigma^2 g^2 \cos^2 \phi} \left[ N - \frac{e^{j(2\theta+2\phi)}}{2} D_N^- - \frac{e^{-j(2\theta+2\phi)}}{2} D_N^+ \right], \\ B_{12} &= \frac{A^2}{2\sigma^2 g \cos^2 \phi} \left[ \frac{e^{j(2\theta+2\phi-\frac{\pi}{2})}}{2} D_N^- + \frac{e^{-j(2\theta+2\phi-\frac{\pi}{2})}}{2} D_N^+ \right], \\ B_{14} &= \frac{AN}{2\sigma^2 g} - \frac{A}{\sigma^2 g \cos \phi} \left[ D_N^- \frac{e^{j(2\theta+\phi)}}{4} + D_N^+ \frac{e^{-j(2\theta+\phi)}}{4} \right], \\ B_{15} &= \frac{A^2 N}{2\sigma^2 g \cos \phi} \left\{ \sin \phi - j \frac{D_N^-}{2N} e^{j(2\theta+\phi)} + j \frac{D_N^+}{2N} e^{-j(2\theta+\phi)} \right\}, \\ B_{22} &= \frac{A^2}{2\sigma^2 \cos^2 \phi} \left[ N + \frac{e^{j(2\theta+2\phi)}}{2} D_N^- + \frac{e^{-j(2\theta+2\phi)}}{2} D_N^+ \right], \\ B_{24} &= -\frac{AN \sin \phi}{2\sigma^2 \cos \phi} - \frac{A}{4\sigma^2 \cos \phi} \left[ D_N^- e^{j(2\theta+\phi+\frac{\pi}{2})} \right. \\ &\quad \left. + D_N^+ e^{-j(2\theta+\phi+\frac{\pi}{2})} \right], \\ B_{25} &= \frac{A^2 N}{2\sigma^2} + \frac{A^2}{4\sigma^2 \cos \phi} \left[ D_N^- e^{j(2\theta+\phi)} + D_N^+ e^{-j(2\theta+\phi)} \right], \end{aligned}$$

$$B_{44} = \frac{N}{\sigma^2}, B_{45} = 0, B_{55} = \frac{A^2 N}{\sigma^2}.$$

Finally,  $D_N^- = D_N(-2\nu_T)$  and  $D_N^+ = D_N(2\nu_T)$  with  $D_N(\nu)$  the Dirichlet function (discrete-time Fourier transform of the causal rectangular window of length  $N$ ).

*Proof:*  $\mathbf{y}$  is a Gaussian vector with expected value  $\mathbf{m} \in \mathbb{R}^{2N \times 1}$  and covariance matrix  $\mathbf{C} \in \mathbb{R}^{2N \times 2N}$ . Moreover, the  $(i, j)$ th term of the Fisher information matrix  $\mathbf{J}$  associated with the probability density function of  $\mathbf{y}$ , say  $J_{ij}$ , is given by [14]

$$J_{ij} = \frac{1}{2} \text{tr} \left( \mathbf{C}^{-1} \frac{\partial \mathbf{C}}{\partial x_i} \mathbf{C}^{-1} \frac{\partial \mathbf{C}}{\partial x_j} \right) + \left( \frac{\partial \mathbf{m}}{\partial x_i} \right)^T \mathbf{C}^{-1} \frac{\partial \mathbf{m}}{\partial x_j} \quad (4)$$

where  $\text{tr}(\cdot)$  is the trace of the matrix argument,  $\mathbf{C}^{-1}$  denotes the inverse of the matrix  $\mathbf{C}$ , and  $x_h$  is the  $h$ th component of the vector  $\mathbf{x} = [g \ \phi \ \sigma^2 \ A \ \theta]^T$ . Thus, letting

$$A_{ij} = \text{tr} \left( \mathbf{C}^{-1} \frac{\partial \mathbf{C}}{\partial x_i} \mathbf{C}^{-1} \frac{\partial \mathbf{C}}{\partial x_j} \right)$$

and

$$B_{ij} = \left( \frac{\partial \mathbf{m}}{\partial x_i} \right)^T \mathbf{C}^{-1} \frac{\partial \mathbf{m}}{\partial x_j}$$

we can compute the terms of Equation (4) and, eventually, prove the theorem. To this end, observe that

$$\mathbf{C} = \text{diag}(\mathbf{C}_0, \dots, \mathbf{C}_0)$$

is the block diagonal matrix with blocks equal to  $\mathbf{C}_0$ , given by

$$\mathbf{C}_0 = \begin{bmatrix} \sigma^2 & g\sigma^2 \sin \phi \\ g\sigma^2 \sin \phi & g^2 \sigma^2 \end{bmatrix},$$

and that  $\mathbf{m}$  can be re-written as

$$\mathbf{m} = [\mathbf{m}^T(0) \cdots \mathbf{m}^T(N-1)]^T,$$

with

$$\mathbf{m}^T(r) = [A \cos(2\pi\nu_T r + \theta) \ Ag \sin(2\pi\nu_T r + \theta + \phi)],$$

$r = 0, \dots, N-1$ . Thus, the elements  $A_{hk}$  of  $\mathbf{A}$  for  $h$  and/or  $k$  greater than 3 are zero since  $\mathbf{C}$  does not depend on  $A$  and  $\theta$ . As to the non-zero terms, they can be easily computed as follows. First notice that

$$\mathbf{C}_0^{-1} = \frac{1}{\sigma^2 g^2 \cos^2 \phi} \begin{bmatrix} g^2 & -g \sin \phi \\ -g \sin \phi & 1 \end{bmatrix};$$

moreover, for instance, we have ( $x_1 \equiv g$ )

$$\frac{\partial \mathbf{C}_0}{\partial x_1} = \sigma^2 \begin{bmatrix} 0 & \sin \phi \\ \sin \phi & 2g \end{bmatrix}$$

and, hence,

$$\mathbf{C}_0^{-1} \frac{\partial \mathbf{C}_0}{\partial x_1} = \frac{1}{g^2 \cos^2 \phi} \begin{bmatrix} -g \sin^2 \phi & -g^2 \sin \phi \\ \sin \phi & 2g - g \sin^2 \phi \end{bmatrix}.$$

Thus,

$$A_{11} = N \text{tr} \left( \mathbf{C}_0^{-1} \frac{\partial \mathbf{C}_0}{\partial x_1} \mathbf{C}_0^{-1} \frac{\partial \mathbf{C}_0}{\partial x_1} \right) = \frac{2N(2 - \sin^2 \phi)}{g^2 \cos^2 \phi}.$$

Similarly, we can compute the non-zero terms of the matrix  $\mathbf{B}$ . For instance, we have that

$$\frac{\partial \mathbf{m}^T(r)}{\partial x_1} = [0 \ A \sin(2\pi\nu_T r + \theta + \phi)].$$

Thus, it follows that

$$\begin{aligned} B_{11} &= \sum_{r=0}^{N-1} \frac{\partial \mathbf{m}^T(r)}{\partial x_1} \mathbf{C}_0^{-1} \frac{\partial \mathbf{m}(r)}{\partial x_1} \\ &= \frac{1}{\sigma^2 g^2 \cos^2 \phi} \sum_{r=0}^{N-1} [0 \ A \sin(2\pi\nu_T r + \theta + \phi)] \\ &\quad \times \begin{bmatrix} g^2 & -g \sin \phi \\ -g \sin \phi & 1 \end{bmatrix} [0 \ A \sin(2\pi\nu_T r + \theta + \phi)]^T \\ &= \frac{A^2}{\sigma^2 g^2 \cos^2 \phi} \sum_{r=0}^{N-1} \sin^2(2\pi\nu_T r + \theta + \phi) \\ &= \frac{A^2}{2\sigma^2 g^2 \cos^2 \phi} \left[ N - \sum_{r=0}^{N-1} \cos(4\pi\nu_T r + 2\theta + 2\phi) \right] \end{aligned}$$

and, finally,

$$\begin{aligned} B_{11} &= \frac{A^2}{2\sigma^2 g^2 \cos^2 \phi} \left[ N - \frac{e^{j(2\theta+2\phi)}}{2} D_N(-2\nu_T) \right. \\ &\quad \left. - \frac{e^{-j(2\theta+2\phi)}}{2} D_N(2\nu_T) \right]. \end{aligned}$$

The other non-zero terms of  $\mathbf{A}$  and  $\mathbf{B}$  can be analogously computed, thus completing the proof. ■

Notice that  $B_{45} = 0$ . Even more important, we can easily compute the  $2 \times 2$  north-west block of the matrix  $\mathbf{J}^{-1}$  and show that it does not depend on  $\theta$ . This result is the object of the next proposition.

*Proposition 3.2:* The matrix  $\mathbf{J}^{-1}$  can be written as

$$\mathbf{J}^{-1} = \begin{bmatrix} \mathbf{D} & \star \\ \star & \star \end{bmatrix}$$

where

$$\mathbf{D} = \begin{bmatrix} D_{11} & D_{12} \\ D_{12} & D_{22} \end{bmatrix}$$

with

$$\begin{aligned} D_{11}^{-1} &= \frac{N(2 - \sin^2 \phi)}{g^2 \cos^2 \phi} + \frac{A^2 N}{2\sigma^2 g^2 \cos^2 \phi} - \frac{N}{g^2} \\ &\quad - \frac{A^2 D_N^- D_N^+}{4N\sigma^2 g^2 \cos^2 \phi} - \frac{A^2 N}{4\sigma^2 g^2} - \frac{A^2 N}{4\sigma^2 g^2} \tan^2 \phi \\ &= \frac{N}{g^2 \cos^2 \phi} + \frac{A^2 N}{4\sigma^2 g^2 \cos^2 \phi} \left( 1 - \frac{D_N^- D_N^+}{N^2} \right) \quad (5) \end{aligned}$$

$$\begin{aligned} D_{22}^{-1} &= \frac{N(1 + \sin^2 \phi)}{\cos^2 \phi} + \frac{A^2 N}{2\sigma^2 \cos^2 \phi} - N \tan^2 \phi \quad (6) \\ &\quad - \frac{A^2 N}{4\sigma^2} \tan^2 \phi - \frac{A^2 N}{4\sigma^2} - \frac{A^2 D_N^- D_N^+}{4N\sigma^2 \cos^2 \phi} = g^2 D_{11}^{-1}, \end{aligned}$$

$$D_{12} = 0,$$

while the  $\star$  denote submatrices of proper dimensions. Finally, we remember that  $D_N^- = D_N(-2\nu_T)$  and  $D_N^+ = D_N(2\nu_T)$  with  $D_N(\nu)$  the Dirichlet function.

*Proof:* It is sufficient to decompose the matrix  $\mathbf{J} \in \mathbb{R}^{5 \times 5}$  as

$$\mathbf{J} = \begin{bmatrix} \mathbf{J}_{11} & \mathbf{J}_{12} \\ \mathbf{J}_{21} & \mathbf{J}_{22} \end{bmatrix},$$

with  $\mathbf{J}_{11} \in \mathbb{R}^{2 \times 2}$ ,  $\mathbf{J}_{12} \in \mathbb{R}^{2 \times 3}$ ,  $\mathbf{J}_{21} \in \mathbb{R}^{3 \times 2}$ , and  $\mathbf{J}_{22} \in \mathbb{R}^{3 \times 3}$ , and compute the  $2 \times 2$  north-west block of its inverse as [14]

$$\mathbf{D} = (\mathbf{J}_{11} - \mathbf{J}_{12}\mathbf{J}_{22}^{-1}\mathbf{J}_{21})^{-1}.$$

It turns out that the off-diagonal terms of  $\mathbf{E} = \mathbf{J}_{11} - \mathbf{J}_{12}\mathbf{J}_{22}^{-1}\mathbf{J}_{21}$ , say  $E_{12}$  and  $E_{21}$ , are zero. In fact, we have that

$$\begin{aligned} E_{12} &= E_{21} = \frac{1}{2}A_{12} + B_{12} - \frac{1}{2}\frac{A_{13}A_{23}}{A_{33}} - \frac{B_{14}B_{24}}{B_{44}} \\ &\quad - \frac{B_{15}B_{25}}{B_{55}} = 0. \end{aligned}$$

Thus, it also follows that the diagonal terms of  $\mathbf{E}$ , say  $E_{11}$  and  $E_{22}$ , are the inverse of  $D_{11}$  and  $D_{22}$ , respectively. Moreover,

$$E_{11} = \frac{1}{2}A_{11} + B_{11} - \frac{1}{2}\frac{A_{13}^2}{A_{33}} - \frac{B_{14}^2}{B_{44}} - \frac{B_{15}^2}{B_{55}}$$

and

$$E_{22} = \frac{1}{2}A_{22} + B_{22} - \frac{1}{2}\frac{A_{23}^2}{A_{33}} - \frac{B_{24}^2}{B_{44}} - \frac{B_{25}^2}{B_{55}}.$$

Computation of  $E_{11}$  and  $E_{22}$  is tedious, but straightforward, and returns Equations (5) and (7). ■

Notice that  $D_{11}$  and  $D_{22}$  do depend on  $\nu_T$  through a term proportional to  $D_N^- D_N^+ / N^2$ ; however, for large values of  $N$  and  $\nu_T$  not too close to zero such term can be neglected. Finally, if  $\nu_T = 0$ , the second addend at the right-hand-side of Equation (5) vanishes.

#### IV. PERFORMANCE ANALYSIS

This section uses the computed CRLB as a reference for the performance of the estimators of  $\phi$  and  $g$ , say  $\hat{\phi}$  and  $\hat{g}$ , respectively, considered in [8], [9]. Performance of the estimators have been computed by Monte Carlo simulations. To this end, we assume a stationary radar (with carrier frequency  $f_0 = 24$  GHz) and the presence of a point-like stationary target with (deterministic) amplitude, located at a certain distance  $r_0$  from the radar. In particular, the radar bandwidth is 150 MHz and the transmit frequency is modulated by a linear up and down ramp over an interval of approximately  $T = 34.1$  ms for each ramp. Remember that  $\nu_T = f_T T_s$  and  $f_T = 2\alpha \frac{r_0}{c}$  (for stationary targets). The number of samples per ramp is equal to  $N = 2048$ . The true values of the I and Q imbalance parameters are set to  $g = 1.5$  and  $\phi = 10$  degrees. Finally, we assume  $\sigma^2 = 1$  and consider several values of  $\nu_T$ .

In Figure 2 we plot the sample mean of  $\hat{\phi}$  and  $\hat{g}$  vs the signal-to-noise ratio (SNR) defined as

$$\text{SNR} = \frac{(2a')^2 / 2}{\sigma^2}$$

while Figure 3 reports the root of the sample mean square error (estimated root mean square error (RMSE)) of  $\hat{\phi}$  and  $\hat{g}$  vs the SNR. Both figures are computed over  $10^3$  trials per SNR value. Figures suggest that the considered estimators are unbiased and that they guarantee adequate performances for SNR values greater than 15 dB and values of  $\nu_T$  not too close to zero. In fact, the estimated RMSE of  $\hat{g}$  is close to the corresponding CRLB for values of  $\nu_T$  greater than or equal to  $10^{-2}$ . As to the estimated RMSE of  $\hat{\phi}$ , its distance from the corresponding CRLB is less than 0.5 for SNR values greater than 15 dB and again values of  $\nu_T$  not too close to zero (greater than or equal to  $10^{-2}$ ).

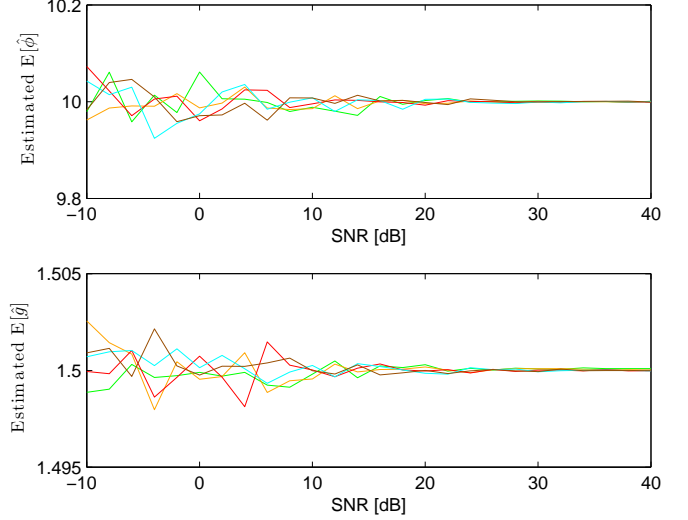


Fig. 2. Estimated values of  $E[\hat{\phi}]$  and  $E[\hat{g}]$  vs the SNR for different values of  $\nu_T$ . Green line:  $\nu_T = 5 \cdot 10^{-3}$ , orange line:  $\nu_T = 7 \cdot 10^{-3}$ , red line:  $\nu_T = 10^{-2}$ , cyan line:  $\nu_T = 5 \cdot 10^{-2}$ , brown line:  $\nu_T = 10^{-1}$ .

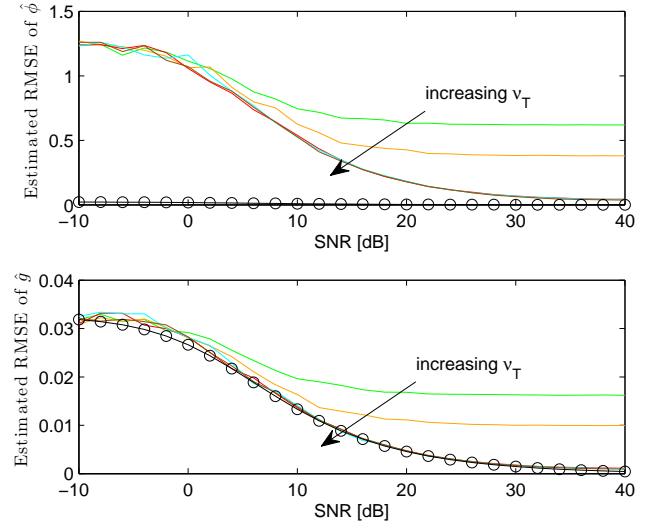


Fig. 3. Estimated values of the RMSE of  $\hat{\phi}$  and  $\hat{g}$  vs the SNR for different values of  $\nu_T$ . Green line:  $\nu_T = 5 \cdot 10^{-3}$ , orange line:  $\nu_T = 7 \cdot 10^{-3}$ , red line:  $\nu_T = 10^{-2}$ , cyan line:  $\nu_T = 5 \cdot 10^{-2}$ , brown line:  $\nu_T = 10^{-1}$ . Black line with circle marker: CRLB for  $\nu_T = 10^{-1}$ .

#### V. CONCLUSIONS

The main result of this paper is the computation of the CRLB for unbiased estimators of I/Q imbalance in presence of nuisance parameters (amplitude and phase of a deterministic sinusoid and the variance of the noise). The extension to the sum of multiple sinusoids (of known frequency) is in principle straightforward, but even more cumbersome. The CRLB has been used to assess performances of already proposed gain and phase estimators by Monte Carlo simulation.

## REFERENCES

- [1] H. Rohling, "Radar CFAR Thresholding in Clutter and Multiple Target Situations", *IEEE Trans. on Aerospace and Electronic Systems*, Vol. 19, No. 4, pp. 608-621, July 1983.
- [2] H. Rohling and R. Mende, "OS CFAR performance in a 77 GHz radar sensor for car application", *CIE International Radar Conference*, Beijing, China, 8-10 October 1996.
- [3] K. Pourvoyeur, R. Feger, S. Schuster, A. Stelzer, and L. Maurer, "Ramp sequence analysis to resolve multi target scenarios for a 77-GHz FMCW radar sensor", *11th International Conference on Information Fusion*, Cologne, Germany, 30 June-3 July 2008.
- [4] F. E. Churchill, G. W. Ogar, and B. J. Thompson, "The Correction of I and Q Errors in a Coherent Processor", *IEEE Trans. on Aerospace and Electronic Systems*, Vol. 17, No. 1, pp. 131-137, January 1981.
- [5] F. E. Churchill, G. W. Ogar, and B. J. Thompson, "Corrections to The Correction of I and Q Errors in a Coherent Processor", *IEEE Trans. on Aerospace and Electronic Systems*, Vol. 17, No. 2, p. 312, March 1981.
- [6] Z. Wang and A. B. Kostinski, "A random wave method for detecting phase imbalance in a coherent radar receiver", *J. of Atmospheric and Oceanic Technology*, Vol. 10, No. 6, pp. 887-891, December 1993.
- [7] M. D. Kulkarni and A. B. Kostinski, "A Simple Formula for Monitoring Quadrature Phase Error with Arbitrary Signals", *IEEE Trans. on Geoscience and Remote Sensing*, Vol. 33, No. 3, pp. 799-802, May 1995.
- [8] V. Dodde, A. Masciullo, and G. Ricci, "Adaptive compensation of amplitude and phase conversion errors for FMCW radar signals," *2015 Intelligent Signal Processing*, London, UK, 1-2 December 2015.
- [9] A. Coluccia, V. Dodde, A. Masciullo, and G. Ricci, "Estimation and compensation of I/Q imbalance for FMCW radar receivers," *2016 IEEE Workshop on Statistical Signal Processing (SSP 2016)*, Palma de Mallorca, Spain, 26-29 June 2016.
- [10] L. Anttila, M. Valkama, and M. Renfors, "Blind Moment Estimation Techniques for I/Q Imbalance Compensation in Quadrature Receivers," *The 17th Annual IEEE International Symposium on Personal, Indoor and Mobile Radio Communications (PIMRC'06)*, Helsinki, Finland, 11-14 September 2006.
- [11] L. Anttila, M. Valkama, and M. Renfors, "Circularity-Based I/Q Imbalance Compensation in Wideband Direct-Conversion Receivers," *IEEE Trans. on Vehicular Technology*, Vol. 57, No. 4, pp. 2099-2113, July 2008.
- [12] G. Vallant, M. Epp, W. Schlecker, U. Schneider, L. Anttila, and M. Valkama, "Analog IQ Impairments in Zero-IF Radar Receivers: Analysis, Measurements and Digital Compensation," *2012 IEEE International Instrumentation and Measurement Technology Conference (I2MTC)*, Graz, Austria, 13-16 May 2012.
- [13] A. G. Stove, "Linear FMCW radar techniques", *IEE Proceedings-F*, Vol. 139, No. 5, pp. 343-350, October 1992.
- [14] L. L. Scharf, *Statistical Signal Processing: Detection, Estimation, and Time Series Analysis*, Addison-Wesley, 1991.